Structure of coherent columnar vortices in three-dimensional rotating turbulent flow

I. V. Kolokolov,[1,2] L. L. Ogorodnikov,[2] and S. S. Vergeles[1,2,*]
[1]*Landau Institute for Theoretical Physics, Russian Academy of Sciences, 1-A Akademika Semenova av., 142432 Chernogolovka, Russia*
[2]*National Research University Higher School of Economics, Faculty of Physics, Myasnitskaya 20, 101000 Moscow, Russia*

(Received 6 October 2019; accepted 20 February 2020; published 30 March 2020)

It is known that the turbulence in a fast-rotating volume becomes effectively two-dimensional. The latter is characterized by an inverse energy cascade leading to the formation of coherent flow in finite systems. In a rotating three-dimensional vessel this flow has the form of columnar vortices. Here we develop an analytical theory describing interaction of the vortex with turbulent pulsations. This interaction results in energy transfer from small-scale eddies to the large-scale vortex. We derive the equation for the radial velocity profile of the vortex and solve it for the simplest boundary conditions. We indicate the domain of physical parameters where our theory works.

DOI: 10.1103/PhysRevFluids.5.034604

I. INTRODUCTION

Fluid flow at large Reynolds numbers is nonstationary and should be described within a statistical approach. The first successful theory was built by Kolmogorov for statistically isotropic three-dimensional (3D) developed turbulent flow. The theory established scaling laws based on direct energy cascade within inertial interval of scales; see Ref. [1]. Direct energy cascade implies that large eddies split into smaller eddies and so on.

Two-dimensional (2D) turbulence, in contrast, is characterized by inverse energy cascade, when small eddies join together to form larger eddies [2]. Bounded 2D flow is of particular physical interest. If the bottom friction is small enough, the size of the largest eddies is limited by the size L of the cell, and large-scale coherent vortices are formed [3,4]. The kinetic energy dissipation due to the bottom friction inside a coherent vortex is compensated by direct energy transfer from small-scale eddies to the vortex in this case, in contrast to the local in scales energy cascade, which is in unbounded systems. The relatively small amplitude of fluctuations compared with the coherent component of the flow allows one to build an analytical theory of the vortices structure [5,6]. The theoretical predictions were recently experimentally verified for the first time [7].

The 2D flow is usually a simplified model of 3D flow that has a suppressed third velocity component. The suppression can be forced for geometric reasons when the third direction is restricted by a scale that is smaller than the scale of the lateral flow (see, e.g., numerical simulations [8] and [9,10], where coherent vortices were observed). For instance, this concerns experiments with excitation of turbulence in thin fluid layers [7,11]. The theory developed for the 2D case can be applied almost directly. The suppression of the third velocity component can be caused by rotation and thus is not associated with geometrical factors [12]. The Taylor-Proudman theorem states that the velocity of the fluid becomes constant along the rotation axis at low Rossby numbers due to

*Corresponding author: ssver@itp.ac.ru

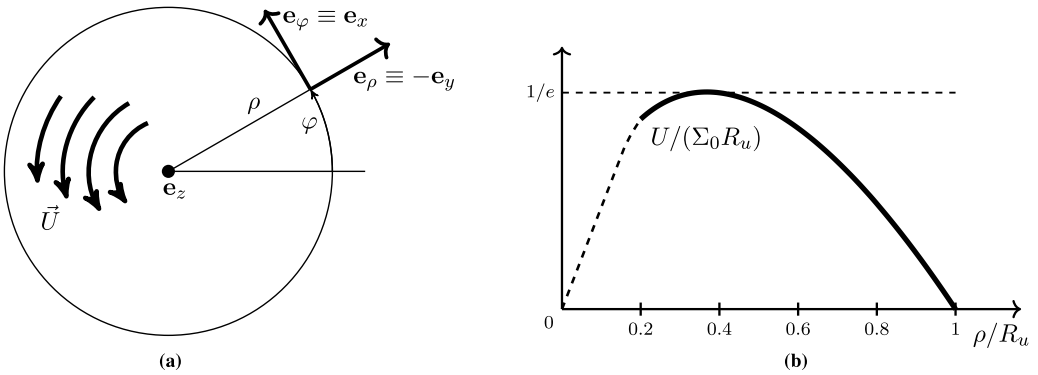

FIG. 1. (a) Vortex scheme and reference systems. (b) The radial profile azimuthal velocity U for $\Sigma = -\Sigma_0$. The dashed line corresponds to the region of the vortex core, $\rho \lesssim r_u$, where the curve is a hypothetical. It was taken as $R_u/r_u \approx 5$.

the Coriolis forces. As a result, the lateral flow and the flow along the z-axis (the axis of rotation) become uncoupled. In particular, the case is believed to be realized inside the Earth's fluid outer core (see, e.g., [13]).

In the paper, we investigate a coherent columnar vortex at low Rossby and high Reynolds numbers. Such vortices were observed in recent direct numerical simulation [14,15] at strong enough forcing. It was checked experimentally that the evolution of the inertial waves is uncoupled from the large-scale two-dimensionalized flow [16] created by the inverse energy cascade [17] and having a form of large-scale columnar vortices [18]. Before that, inverse energy cascade along with direct cascade in the sector of inertial waves was observed in numerical simulation [19] at moderate low Rossby number. In our investigation, the small-scale inertial waves are assumed to be excited by a random small-scale force with homogeneous statistics in time and space. The inertial waves are affected by local shear flow produced by the differential rotation in the vortex before they die out due to viscosity. We show that the shear flow influence leads to a strong anisotropy of the wave statistics and in particular to the wave energy being transferred to the vortex. We establish the equation governing the radial mean velocity profile in the vortex and find the profile.

II. THE MODEL

We assume that the fluid is rotating as a whole with angular velocity $\mathbf{\Omega}$. In the rotating frame, the Navier-Stokes equation acquires an additional term describing Coriolis forces,

$$\partial_t \boldsymbol{v} + (\boldsymbol{v}, \nabla)\boldsymbol{v} + 2[\mathbf{\Omega} \times \boldsymbol{v}] = -\nabla p + \nu \Delta \boldsymbol{v} + \boldsymbol{f}. \tag{1}$$

The fluid is incompressible, so $\operatorname{div} \boldsymbol{v} = \mathbf{0}$. In (1), p is the effective pressure divided by the fluid mass density, which differs from the physical pressure by addition of the potential produced by the centrifugal forces. We divide the full velocity field $\boldsymbol{v}$ into large-scale and slowly varying in time velocity $\boldsymbol{U}$ describing the coherent vortex and the small-scale rapidly varying in time turbulent pulsations $\boldsymbol{u}$, $\boldsymbol{v} = \boldsymbol{U} + \boldsymbol{u}$. The coherent vortex is assumed to be homogeneous along the rotation axis and axially symmetric; its axis is parallel to the rotation direction. We refer to the vortex as columnar. We introduce a cylindrical reference frame $\{\rho, \varphi, z\}$ with the z-axis coinciding with the vortex axis; see Fig. 1(a). Thus the vortex has only an azimuthal velocity component, which we denote by U including the sign. By definition, the temporal mean value of the small-scale component $\boldsymbol{u}$ is zero. It is excited by a random force $\boldsymbol{f}$ with zero mean value. The force produces the energy flux per unit mass ϵ, has a correlation length in space equal to $1/k_f$, and is assumed to be shortly correlated in

time. We model the force to be statistically homogeneous in time and space:

$$\left\langle f^i_{\mathbf{k}}(t)\, f^j_{\mathbf{q}}(t_1)\right\rangle \;=\; (2\pi)^3\left(\delta^{ij}-\frac{k^i k^j}{\mathbf{k}^2}\right)\epsilon\,\delta(\mathbf{k}+\mathbf{q})\delta(t-t_1)\chi(\mathbf{k}), \qquad \int\frac{\chi(\mathbf{k})d^3k}{(2\pi)^3}=1, \tag{2}$$

where, e.g., $\mathbf{k}$ is the wave vector in Fourier space, so $f^i_{\mathbf{k}}=\int d^3r\,\exp(-i\mathbf{k}\cdot\boldsymbol{r})f^i(\boldsymbol{r})$. The characteristic radius of the vortex R_u is assumed to be large compared to the force scale, $k_f R_u \gg 1$. We choose the Gaussian spatial profile for the correlation function,

$$\chi(\mathbf{k}) \;=\; \frac{16\pi^{3/2}}{3k_f^5}\,k^2\exp\left(-\frac{k^2}{k_f^2}\right), \tag{3}$$

to elucidate analytical calculations up to final estimates.

The Navier-Stokes equation averaged over fast small-scale velocity pulsations leads to the equation for the mean vortex velocity,

$$\partial_t U=-\left(\partial_\rho+\frac{2}{\rho}\right)\Pi^{\varphi\rho},\qquad \Pi^{\varphi\rho}=\langle u^\rho u^\varphi\rangle-\nu\Sigma. \tag{4}$$

Here, u^ρ and u^φ are the projections of the velocity field $\boldsymbol{u}$ on local orthonormal basis vectors $\mathbf{e}_\rho$ and $\mathbf{e}_\varphi$, respectively [see Fig. 1(a)], $\Sigma=\rho\partial_\rho(U/\rho)$ is the local large-scale shear rate, and $\Pi^{\varphi\rho}$ is the mean value of the φ-component of momentum flux per unit mass in the radial direction. In other words, $\Pi^{\varphi\rho}(\rho_0)$ is the tangent force applied at the surface $\rho=\rho_0$. In particular, the average $\langle u^\rho u^\varphi\rangle$ is the Reynolds stress contribution into the flux. Equation (4) differs from that for the two-dimensional vortex by the absence of bottom friction [5]. In what follows, we consider the stationary limit when $\partial_t U=0$. Then, the momentum flux $\Pi^{\varphi\rho}$ should be zero because $-\rho_0^2\Pi^{\varphi\rho}(\rho_0)$ is the torque (per unit length in the z-direction), which acts on the fluid inside the circle, $\rho<\rho_0$, and the stationarity implies that it is equal to zero. Thus, the equation governing the vortex velocity profile has the form

$$\Pi^{\varphi\rho}=\langle u^\rho u^\varphi\rangle-\nu\Sigma=0. \tag{5}$$

Now let us consider the evolution of the pulsating component of the flow $\boldsymbol{u}$. Assuming that both the Coriolis force and the interaction of the pulsations with the coherent flow $\boldsymbol{U}$ exceed self-nonlinearity, we linearize the Navier-Stokes equation with respect to $\boldsymbol{u}$:

$$\partial_t\boldsymbol{u}+(\boldsymbol{U}\nabla)\boldsymbol{u}+(\boldsymbol{u}\nabla)\boldsymbol{U}+2[\boldsymbol{\Omega}\times\boldsymbol{u}]=-\nabla p+\nu\Delta\boldsymbol{u}+\boldsymbol{f}. \tag{6}$$

Here p is a fluctuating part of the pressure. Consider some Lagrangian trajectory in the mean flow, which is $\varphi(t)=tU(\rho_0)+\varphi_0$, $z=z_0$. Because the velocity pulsations are assumed to be small-scale, one can consider the evolution of the pulsations locally in the vicinity of the Lagrangian trajectory, when $|\rho-\rho_0|\ll\rho_0$. To exploit the approximation, we go into the new reference frame that moves with the Lagrangian trajectory and rotates with angular velocity $U(\rho_0)/\rho_0$ around the z-axis. We consider the limit of small Rossby number $\mathrm{Ro}_\kappa\ll 1$ for the large-scale vortex, which implies $U/\rho\ll\Omega$. In the reference frame, we choose Cartesian coordinates $\{x,y,z\}$ as depicted in Fig. 1(a); note that the basis vectors of the Cartesian coordinates form a right triad. The mean velocity profile in the neighborhood can be approximated as a linear shear flow, $U^x=-\Sigma y$. Thus, Eq. (6) can be rewritten in the form

$$(\partial_t-\Sigma y\partial_x)\boldsymbol{u}-u^y\Sigma\mathbf{e}_x+2\Omega[\mathbf{e}_z\times\boldsymbol{u}]=-\nabla p+\nu\Delta\boldsymbol{u}+\boldsymbol{f}, \tag{7}$$

where $\Sigma=\Sigma(\rho_0)$. To be accurate, Ω should be substituted by $\Omega+U(\rho_0)/\rho_0$ in Eq. (7), but the assumed small Rossby number causes the correction to be negligible. The smallness of the correction means that there is no difference between cyclones and anticyclones in this limit. The equation is convenient to solve in Fourier space,

$$(\partial_t+\Sigma k_x\partial_{k_y})\boldsymbol{u}_{\mathbf{k}}=-2\Omega[\mathbf{e}_z\times\boldsymbol{u}_{\mathbf{k}}]+\Sigma u^y_{\mathbf{k}}\mathbf{e}_x-i\mathbf{k}p_{\mathbf{k}}-\nu\mathbf{k}^2\boldsymbol{u}_{\mathbf{k}}+\boldsymbol{f}_{\mathbf{k}}. \tag{8}$$

A low Rossby number Ro_κ for the large-scale flow assumes that $\Sigma\ll\Omega$.

III. DYNAMICS OF SMALL-SCALE EDDIES

First consider a homogeneous version of Eq. (8), that is, without force. The main term is the Coriolis force, which leads to inertial wave oscillations [20]. The oscillations are described in terms of two circular polarizations,

$$\boldsymbol{u}_{\mathbf{k}} = \sum_{s=\pm 1} a_{\mathbf{k}s}\boldsymbol{h}^s_{\mathbf{k}}, \quad \boldsymbol{h}^s_{\mathbf{k}} = \frac{[\mathbf{k}\times[\mathbf{k}\times\boldsymbol{e}_z]] - isk[\mathbf{k}\times\boldsymbol{e}_z]}{\sqrt{2}\,kk_\perp}, \tag{9}$$

where $k_\perp = \sqrt{k_x^2 + k_y^2}$. The basis vectors $\boldsymbol{h}^s_{\mathbf{k}}$ satisfy the normalization condition and the symmetry relations:

$$\left(\boldsymbol{h}^{-s}_{\mathbf{k}}, \boldsymbol{h}^s_{\mathbf{k}}\right) = 1, \quad \left(\boldsymbol{h}^s_{\mathbf{k}}, \boldsymbol{h}^s_{\mathbf{k}}\right) = 0, \quad \boldsymbol{h}^{*,s}_{\mathbf{k}} = \boldsymbol{h}^{-s}_{\mathbf{k}} = \boldsymbol{h}^s_{-\mathbf{k}}, \tag{10}$$

where an asterisk denotes complex conjugation. If only the Coriolis force is acting, the dynamics of wave amplitude $a_{\mathbf{k}s}$ is governed by the equations

$$\partial_t a_{\mathbf{k}s} = is\omega_{\mathbf{k}} a_{\mathbf{k}s}, \quad \omega_{\mathbf{k}} = 2\Omega(k_z/k). \tag{11}$$

The main influence of the shear flow stems from the left-hand side of (8) and results in moving the wave amplitudes along characteristics in Fourier space:

$$k'_y(t) = k_y + \Sigma t k_x, \quad \mathbf{k}'(t) = \{k_x, k'_y(t), k_z\}. \tag{12}$$

The full equation (8) rewritten based on the characteristics in terms of the wave amplitudes has the form

$$\partial_t a_{\mathbf{k}'s} = \sum_{\sigma=\pm 1} H_{s\sigma}(\mathbf{k}')\, a_{\mathbf{k}'\sigma} - \nu \mathbf{k}'^2 a_{\mathbf{k}'s} + f^s_{\mathbf{k}'}, \tag{13}$$

where the matrix elements of $\hat{H}$ are

$$H^{ss}_{\mathbf{k}} = is(\omega_{\mathbf{k}} + \delta\omega_{\mathbf{k}}) + \ell_{\mathbf{k}}, \quad \ell_{\mathbf{k}} = -\Sigma\frac{k_x k_y}{2k^2}, \quad \delta\omega_{\mathbf{k}} = \Sigma\frac{k_z\left(3k_x^2 + k_y^2\right)}{2kk_\perp^2}, \tag{14}$$

$$H^{-s,s}_{\mathbf{k}} = \Sigma h^{s,x}_{\mathbf{k}} h^{s,y}_{\mathbf{k}} = \Sigma\frac{k_x k_y\left(k^2 + k_z^2\right) + iskk_z\left(k_x^2 - k_y^2\right)}{2k_\perp^2 k^2}. \tag{15}$$

The force statistics (2) leads to the following correlation function of the Fourier components $f^s_{\mathbf{k}}(t)$:

$$\left\langle f^s_{\mathbf{k}}(t_1) f^\sigma_{\mathbf{q}}(t_2)\right\rangle = \epsilon\,(2\pi)^3\delta(\mathbf{k}+\mathbf{q})\,\delta(t_1 - t_2)\chi(\mathbf{k})\,\delta_{s\sigma}. \tag{16}$$

The formal solution of (13) can be written as

$$a_{\mathbf{k}'(t)s}(t) = \int_{-\infty}^{t} d\tau\, \exp\left(-\nu\int_\tau^t dt_1 k'^2(t_1)\right)\sum_\sigma Q^{s\sigma}(t,\tau) f^\sigma_{\mathbf{k}'(\tau)}(\tau), \tag{17}$$

where the evolution matrix $\hat{Q}$ satisfies the equation

$$\partial_t \hat{Q}(t,\tau) = \hat{H}_{\mathbf{k}'(t)}\hat{Q}(t,\tau), \quad Q^{s\sigma}(\tau,\tau) = \delta^{s\sigma}, \tag{18}$$

and it can be formally written as an ordered exponential:

$$\hat{Q}(t,\tau) = \mathcal{T}_{t_1}\exp\left(\int_\tau^t dt_1\,\hat{H}_{\mathbf{k}'(t_1)}\right), \tag{19}$$

where $\mathcal{T}_{t_1}$ denotes antichronological ordering.

Evolution matrix (19) can be expressed in terms of some special functions; see [21]. However, in the limit of small Rossby number, $\mathrm{Ro}_R \sim \Sigma/\Omega \ll 1$ it can be simplified drastically. Indeed, in this case almost all small-scale eddies evolve as superpositions of fast oscillating inertia waves with

$k_z/k \gg \Sigma/\Omega$. The corresponding frequencies $\omega_{\mathbf{k}}$ are much greater than all other contributions in (14). Keeping the zero order in the small parameter $\Sigma k/\Omega k_z$, only diagonal matrix elements should be counted in the matrix $\hat{H}_{\mathbf{k}}$. Then (17) becomes

$$a_{\mathbf{k}'(t)s}(t) = \int_{-\infty}^{t} d\tau \sqrt{\frac{k'(\tau)}{k(t)}} \exp\left(isG_{\mathbf{k}}(t,\tau) - \nu \int_{\tau}^{t} dt_1 k'^2(t_1) \right) f^{s}_{\mathbf{k}'(\tau)}(\tau), \tag{20}$$

where the phase $G_{\mathbf{k}}(t,\tau) = \int_{\tau}^{t} dt_1(\omega_{\mathbf{k}'(t_1)} + \delta\omega_{\mathbf{k}'(t_1)})$. To find expectation values like $\langle u^{\rho}u^{\varphi}\rangle$, the following elementary averages are needed:

$$\langle a^{*}_{\mathbf{k}s} a_{\mathbf{q}\sigma}\rangle = (2\pi)^3 \delta(\mathbf{k}-\mathbf{q}) A_{\mathbf{k}s\sigma}. \tag{21}$$

Using the correlation function of the force (16) and the expression (20) for the wave amplitudes, it can be found that

$$A_{\mathbf{k}ss} = \epsilon \int_{-\infty}^{0} d\tau\, \chi(\mathbf{k}'(\tau)) \frac{k'(\tau)}{k} e^{-2\int_{\tau}^{0} dt_1\, \nu k'^2(t_1)}, \quad A_{\mathbf{k}s,-s} = 0. \tag{22}$$

The diagonal average $A_{\mathbf{k}ss}$ describes the spectrum of the inertial wave ensemble; the off-diagonal average, which characterizes the correlation between waves with opposite polarization, is zero.

The influence produced by off-diagonal matrix elements $H^{s,-s}_{\mathbf{k}}$ on the right-hand side of (13) can be considered as nonresonant perturbation of amplitude $\sim\Sigma$ in terms of quantum mechanics. Such perturbation produces corrections that are relatively small as $\Sigma/\omega_{\mathbf{k}}$. We explicitly show this in Appendix A.

IV. THE STATISTICS OF THE VELOCITY IN SMALL EDDIES

Here we calculate the correlator $\langle u^{\rho}u^{\varphi}\rangle = -\langle u^{x}u^{y}\rangle$, which enters into Eq. (4). Expressions (9) for the components of the basis vectors of the circular polarizations yield

$$-u^{x}_{\mathbf{k}}u^{y}_{-\mathbf{k}} = \sum_{s=\pm1} |a_{\mathbf{k}s}|^2 \frac{k_x k_y + isk k_z}{2k^2} + \frac{2}{\Sigma}\mathrm{Re}(a^{*}_{\mathbf{k},+}a_{\mathbf{k},-}H^{+-}_{\mathbf{k}}). \tag{23}$$

When calculating (23), it should be taken into account that the inertial wave amplitude distribution (21) is symmetric under vertical reflection $k_z \to -k_z$, and the cross-correlations between opposite polarizations are negligible [see Eq. (22)]. As a result,

$$\langle u^{\rho}u^{\varphi}\rangle = \epsilon \int \frac{d^3k}{(2\pi)^3} \int_{-\infty}^{0} d\tau\, \chi(\mathbf{k}'(\tau)) \frac{k_x k_y k'(\tau)}{k^3} \exp\left(-2\nu \int_{\tau}^{0} dt' k'^2(t') \right). \tag{24}$$

The integrand in (24) is very similar to that in the two-dimensional case [5]. It is not an incident, since we have accounted for the same movement along characteristics whereas nonlinear interactions of three-dimensional pulsations are suppressed due to inertial wave oscillations. The difference is in the power of the factor $k'(\tau)/k$, which does not effect the calculation scheme. To evaluate the integral (24), first we choose the dimensionless time variable, $\tau \to -\tau/\Sigma$; then we introduce the parameter $\gamma = 2\nu k_f^2/\Sigma \ll 1$, which characterizes the relative intensity of the viscous dissipation. After that, we proceed to the "reversed" time via the transformation $k_y \to k_y + \tau k_x$. As a result,

$$\langle u^{\rho}u^{\varphi}\rangle = \frac{\epsilon}{\Sigma} \int \frac{k^2 \sin\theta\, dk\, d\theta\, d\phi}{(2\pi)^3} \chi(\mathbf{k}) \int_{0}^{\infty} \frac{d\tau}{2\lambda^{3/2}} \frac{d\lambda}{d\tau} \exp(-\gamma k^2 \Lambda), \tag{25}$$

where $\lambda(\tau) = 1 + \tau\sin^2\theta\sin(2\phi) + (\tau\sin\theta\cos\phi)^2$, $\Lambda(\tau) = \int_0^{\tau}\lambda(\tau')d\tau'$, and θ, ϕ are spherical angles of the wave vector $\mathbf{k}$. Now we integrate by parts over τ, keeping in mind that $\lambda(0) = 1$ and

the normalization condition for $\chi(\mathbf{k})$ (2):

$$\langle u^\rho u^\varphi \rangle = \frac{\epsilon}{\Sigma}\left(1 - \gamma\frac{5}{8\pi}\int_0^\pi \sin\theta\, d\theta \int_0^{2\pi} d\phi \int_0^\infty \frac{\sqrt{\lambda}\, d\tau}{(1+\gamma\Lambda)^{7/2}}\right) \approx \frac{\epsilon}{\Sigma}. \tag{26}$$

For the latter integral, we have used a particular form of the spatial profile for the force correlation function (3) and integrated over k. The integral only produces a correction that is relatively as small as $\gamma^{1/3}$; see (B7) in Appendix B. Note that the main part of the integral (25) is accumulated at a timescale $t \sim 1/\Sigma$ (that is, $\tau \sim 1$ in terms of the dimensionless time); see Eqs. (B3) and (B4) in Appendix B. This is a significant difference from the two-dimensional case, where the Reynolds stress is determined by the timescale $t \sim t_* = (\nu k_f^2 \Sigma^2)^{-1/3}$ [5] (that is, $\tau \sim \tau_* = \gamma^{-1/3}$ in terms of the dimensionless time).

The unaccounted for nonlinear interaction between the small-scale eddies is irrelevant for Reynolds stress (25) because the stress is formed on the time interval of the order of $\sim 1/\Sigma$. Indeed, the nonlinear interaction of inertial waves is determined by the omitted term $(\boldsymbol{u}\nabla)\boldsymbol{u}$ in (6), the relative amplitude of which can be estimated as $k_f u$. The fast inertial wave oscillations suppress the nonlinear interaction, so it becomes important at times $t_{\rm tr} \sim \Omega/(k_f u)^2$ [22]. The relative impact of the nonlinear interaction on the mean (26) is $1/\Sigma t_{\rm tr} \sim k_f^2 u^2/\Sigma\Omega$. It can be found in a similar way to how (26) was obtained that $\langle \boldsymbol{u}^2 \rangle \sim (\epsilon/\Sigma)\ln^2(\Sigma/\nu k_f^2)$; see (B11) in Appendix B. Below it is shown that $\Sigma \sim \sqrt{\epsilon/\nu}$. Hence, the relative impact is small, being of the order of a small Ekman number ${\rm Ek} = \nu k_f^2/\Omega \ll 1$. Thus, the constructed analysis of the Reynolds stress component is self-consistent.

If the shear rate Σ becomes small enough, the evaluation (26) is not valid anymore. Instead, inertial waves should be considered to form isotropic weak turbulence with the spectrum $E(k) \sim \sqrt{\Omega\epsilon}/k^2$ [23,24], which implies the estimation $\langle \boldsymbol{u}^2 \rangle \sim \sqrt{\Omega\epsilon}/k_f$. The isotropic turbulence is established if the energy transition rate $1/t_{\rm tr} \sim k_f\sqrt{\epsilon/\Omega}$ [22] is greater than the shear rate Σ, $\Sigma \ll k_f\sqrt{\epsilon/\Omega}$. Then the shear can be considered as weak perturbation, and the cross-correlation is evaluated as $\langle u^\rho u^\varphi \rangle \sim (\Sigma t_{\rm tr})\langle \boldsymbol{u}^2 \rangle \sim \Sigma\Omega/k_f^2$.

It is also worth mentioning that the presented calculations (20)–(26) do not account for the quasi-two-dimensional sector of the eddy pulsations that are characterized by wave vectors with $k_z \lesssim (\Sigma/\Omega)k_x$. However, the relative fraction in wave-vector space of the pulsations is as small as Σ/Ω. This estimate is valid for the relative contribution into the cross-correlation $\langle u^\rho u^\varphi \rangle$ as well.

V. MEAN VELOCITY RADIAL PROFILE

First, let us evaluate power P (linear density along the z-axis), which is transmitted from the small-scale eddies to the vortex flow. It is

$$P = -2\pi\int_0^{R_u} \rho U\left(\partial_\rho + \frac{2}{\rho}\right)\langle u^\rho u^\varphi\rangle d\rho = 2\pi\int_0^{R_u} \Sigma\langle u^\rho u^\varphi\rangle\, \rho\, d\rho - 2\pi\rho U\langle u^\rho u^\varphi\rangle\Big|_0^{R_u} \tag{27}$$

according to (4), where R_u is some fixed radius. Suppose that the shear rate Σ is strong enough that estimate (26) is valid over a major part of the region $\rho < R_u$. Then the first term on the right-hand side of (27) approaches $\pi R_u^2\epsilon$ from below, i.e., almost all of the power is produced inside the region by the random force (2). Here we note that the sign of the cross-correlation (26) is opposite to the sign of the cross-correlation for simple shear flow without rotation [25]. According to (27), this difference corresponds to the difference in energy transfer: the transfer is directed from large-scale flow to small-scale fluctuations in the simple shear flow. The other term on the right-hand side of (27) should be treated as a power flux that comes into the region from outside. So if we now call R_u the vortex radius, it would be reasonable to suppose that the product $U\langle u^\rho u^\varphi\rangle$ becomes zero at the vortex boundary $\rho = R_u$. This can be due to either U or the shear rate Σ or both of them dropping to zero at the boundary.

In the region where (26) is valid, the solution of stationary equation (5) is $\Sigma = \pm\Sigma_0$, where $\Sigma_0 = \sqrt{\epsilon/\nu}$. Our theory is valid if the Rossby number $\mathrm{Ro}_\kappa \sim \Sigma_0/\Omega$ characterizing the large-scale flow is small, that is, $\mathrm{Ro}_\kappa \sim \mathrm{Ro}_f\sqrt{\mathrm{Re}_f} \ll 1$ [14], where the Rossby and Reynolds numbers for the pumping are $\mathrm{Ro}_f = (\epsilon k_f^2)^{1/3}/\Omega$ and $\mathrm{Re}_f = (\epsilon/k_f^4)^{1/3}/\nu$ by definition. The solution for U should satisfy the condition $U = 0$ at the vortex boundary $\rho = R_u$. Then the energy flux indeed turns to zero at the boundary:

$$U(\rho) = \pm\rho \int_{R_u}^{\rho} d\rho' \frac{\Sigma_0}{\rho'} = \mp\rho\Sigma_0 \ln\frac{R_u}{\rho}. \tag{28}$$

Since the logarithm (28) is always positive at $\rho < R_u$, the first and second choices of sign in (28) correspond to anticyclone and cyclone, respectively. There is a symmetry between them in the considered limit of fast rotation. The relative correction to the vortex profile (28) due to the finiteness of the Rossby number is of the order of Σ_0/Ω; see (A3). These corrections should reveal a weak difference between cyclones and anticyclones. The form of the profile of U is universal, and it is plotted in Fig. 1(b). Note that the integral vorticity that is associated with the vortex is zero. Indeed, the z-component of vorticity is $\omega_z = (1/\rho)\partial_\rho(\rho U) = \mp\Sigma_0[2\ln(R_u/\rho) - 1]$. Then the integral vorticity is $\int_0^{R_u} \partial_\rho(\rho U)\, d\rho = 0$.

The necessary condition for the expression (28) to be valid is $\rho k_f \gg 1$. However, the local shear approximation used in (8) ceases to work at larger radius r_u due to the spreading of inertial waves excited by the pumping. The value of the core size r_u can be found as the product of the characteristic time $\sim 1/\Sigma$ with the group velocity of the inertial waves $v_g \sim \Omega/k_f$, which leads to the estimation $r_u \sim k_f^{-1}/\mathrm{Ro}_\kappa$. At $\rho \ll r_u$, this smearing of the pumping effect leads to the diminishing of Σ and analyticity of the function $U(\rho)$. The precise shape of $U(\rho)$ in this small-ρ region is beyond the scope of this paper.

VI. CONCLUSION

We have presented an analytical theory that shows how inertial wave turbulence in rotating fluid transfers its energy to a large-scale columnar vortex. Inertial waves excited by a small-scale force donate almost all their kinetic energy to the vortex so that the vortices quickly disappear, and there is no time to waste the energy into heat under the action of the viscosity. In this sense, the energy transfer efficiency from the small-scale force to the large-scale coherent flow approaches unity.

The presented theory is correct only in the limit of a rapidly rotating fluid. In the limit, there is symmetry between cyclones and anticyclones. The symmetry was observed in numerical simulation [14], where the limit was called a "viscous condensate" and it reached $\mathrm{Ro}_\kappa \approx 0.2$. The considerable difference between cyclones and anticyclones arises if the ratio of the local shear parameter to the rotation frequency Σ/Ω becomes of the order of 1. This is the case of, e.g., the experimental work of Ref. [18], where $\mathrm{Ro}^{(l)}\sqrt{\mathrm{Re}^{(l)}} \geqslant 1.6$, and the numerical simulation of Ref. [15], where $\mathrm{Ro}_\kappa = u_0^2/(\Omega\nu\sqrt{\mathrm{Re}_\lambda}) \gtrsim 10$. To describe the regime, one should solve the evolution equation (13), taking into account the strong coupling between inertia waves with opposite circular polarizations.

Summing up, we conclude that the coherent vortex is the result of (i) the existence of inertia waves and their uncoupling from quasi-two-dimensional flow under the action of rotation, and (ii) inverse energy cascade, which is locked at scales of the order of the cell size L [14], as it is in pure two-dimensional flow [4]. Then the vortex size R_u should be of the order of L. The statement is in agreement with numerical simulation [14], where it was observed that one cyclone and anticyclone pair occupies the whole cell. Our theory, which is based on the local shear approximation, is valid if $k_f R_u \gg 1/\mathrm{Ro}_f\sqrt{\mathrm{Re}_f}$. In other words, the scale $1/k_f$ of the random force should be quite small. For example, the parameters used in [14] are close to this requirement, since $Lk_f \approx 25$ in the case. If the requirement is not fulfilled, the eddies cannot be treated as small-scale, and the local shear approximation (7) is not applicable anymore. The development of a rapid distortion theory on a background of nonuniform large-scale velocity is needed to describe the statistics of the eddies in

this case. As an example, this was done in [26] for the particular case of the vortex profile $U \propto 1/\rho$ in the limit of weak backreaction of the turbulent pulsations onto the mean flow.

ACKNOWLEDGMENTS

I.K. acknowledges Russian Ministry of Science and High Education. L.L. and S.V. prepared the publication within the framework of the Academic Fund Program at the National Research University Higher School of Economics (HSE) in 2019 (Grant No.19-04-015) and within the framework of the Russian Academic Excellence Project "5-100" and were supported by Grant No. 19-1-2-46-1 of Foundation for the Advancement of Theoretical Physics and Mathematics "BASIS."

APPENDIX A: EVALUATION OF THE CORRECTIONS INTO THE CORRELATION FUNCTIONS

Here we show explicitly that off-diagonal matrix elements $H_{\mathbf{k}}^{s,-s}$ in (14) produce a correction in (22) that is relatively as small as $\Sigma k/\Omega k_z$. For this purpose, let us extract in $\hat{Q}$ (19) the unperturbed evolution factor corresponding to zero off-diagonal terms:

$$Q_{\mathbf{k}}^{s\sigma}(t,\tau) = \exp(isG_{\mathbf{k}}(t,\tau))P_{\mathbf{k}}^{s\sigma}(t,\tau). \tag{A1}$$

The evolution equation on the introduced matrix $\hat{P}_{\mathbf{k}}(t,\tau)$ is

$$\partial_t \hat{P}_{\mathbf{k}}(t,\tau) = \begin{pmatrix} 0 & B_{\mathbf{k}}(t,\tau) \\ B_{\mathbf{k}}^*(t,\tau) & 0 \end{pmatrix} \hat{P}_{\mathbf{k}}(t,\tau), \quad P_{\mathbf{k}}^{s\sigma}(\tau,\tau) = \delta^{s\sigma}, \tag{A2}$$

where $B_{\mathbf{k}}(t,\tau) = H_{\mathbf{k}(t)}^{+-}\exp(-2iG_{\mathbf{k}}(t,\tau))$. The off-diagonal element of matrix $\hat{P}_{\mathbf{k}}$ is approximately equal to the result of the first iteration of the solution of Eq. (A2),

$$P_{\mathbf{k}}^{+-}(t,\tau) = \int_\tau^t B_{\mathbf{k}}(t_1,\tau)dt_1 \approx \frac{iH_{\mathbf{k}(t)}^{+-}}{2\omega_{\mathbf{k}(t)}} - \frac{iH_{\mathbf{k}(\tau)}^{+-}}{2\omega_{\mathbf{k}(\tau)}} \sim \frac{\Sigma k}{\Omega k_z}, \tag{A3}$$

due to the integrand containing a fast oscillating factor. To find the correction to the diagonal element of matrix $\hat{P}_{\mathbf{k}}$, the next iteration should be implemented in the solution of (A2), which is based on the result of the previous iteration (A3). Thus, the correction is of the order of $\Sigma k/\Omega k_z$ as well.

APPENDIX B: CALCULATIONS OF THE REYNOLDS STRESS

Here we demonstrate the calculations of pair averages $\langle u^\rho u^\varphi\rangle$ and $\langle \boldsymbol{u}^2\rangle$ in detail. In particular, we find out the convergence rate of the integrals in inverse time τ; see (25) and (26). Our analysis will use the asymptotic behavior of functions $\lambda(\tau)$ and $1+\gamma\Lambda(\tau)$ at large $\tau \gg 1$ and when $|\cos\phi| \ll 1$. In the limit, one has for $\lambda(\tau)$

$$\lambda(\tau) = \cos^2\theta + \sin^2\theta\left(\frac{\sin^2\phi}{\tau^2+1} + \left(\sqrt{\tau^2+1}\cos\phi + \frac{\tau\sin\phi}{\sqrt{\tau^2+1}}\right)^2\right) \approx \cos^2\theta(1+\zeta^2), \tag{B1}$$

$$\zeta = \tan\theta\left(\sqrt{\tau^2+1}\cos\phi + \frac{\tau\sin\phi}{\sqrt{\tau^2+1}}\right) \approx \tan\theta(\tau\cos\phi + \sin\phi).$$

We need a combination of $1+\gamma\Lambda$; see (26). In the limit $\tau \gg 1$ and $|\cos\phi| \ll 1$,

$$\begin{aligned} 1+\gamma\Lambda &= 1+\gamma\tau+\gamma\tau\sin^2\theta\left(\frac{\tau\sin(2\phi)}{2} + \frac{\tau^2\cos^2\phi}{3}\right) \\ &\approx 1 + \frac{\gamma\tau(3\cos^2\theta+\sin^2\theta)}{4} + \frac{\gamma\tau\cos^2\theta}{3}\left(\zeta + \frac{\tan\theta}{2}\right)^2. \end{aligned} \tag{B2}$$

Note that $\gamma\Lambda \ll 1$ at all angles if $\tau \ll \tau_*$ with $\tau_* = \gamma^{-1/3}$.

First we start from Reynolds stress $\langle u^\rho u^\varphi \rangle$ (25). To find the characteristic timescale where the integral is converged, consider its residue that is the part of the integral in (25) over the time interval $T < \tau \lesssim \infty$:

$$\frac{\epsilon}{\Sigma}\int \frac{d^3k}{(2\pi)^3}\chi(\mathbf{k})\int_T^\infty d\tau\,\frac{d\lambda/d\tau}{2\lambda^{3/2}} = \frac{\epsilon}{\Sigma}\int \frac{d^3k}{(2\pi)^3}\chi(\mathbf{k})\left(\frac{e^{-\gamma k^2\Lambda(T)}}{\sqrt{\lambda(T)}} - \gamma k^2\int_T^\infty d\tau\sqrt{\lambda}e^{-\gamma k^2\Lambda}\right). \tag{B3}$$

The exponent in (B3) is unity for $k \lesssim k_f$ at times $1 \ll T \ll \tau_*$ in the first summand on the right-hand side of (B3). Now assume for simplification that $\chi(\mathbf{k})$ is isotropic and depends only on the absolute value of the wave number k. Then the first summand on the right-hand side of (B3) is estimated as

$$\frac{\epsilon}{\Sigma}\int_0^\pi \frac{d\theta}{4\pi T}\int_0^{2\pi}\frac{T|\tan\theta|\,d\phi}{\sqrt{1+\zeta^2}} \sim \frac{\epsilon}{\Sigma}\int_0^\pi \frac{d\theta}{\pi T}\int_0^{\sim T|\tan\theta|}\frac{d\zeta}{\sqrt{1+\zeta^2}}$$
$$\sim \frac{\epsilon}{\Sigma T}\int_0^\pi \frac{d\theta}{\pi}\ln(T|\tan\theta|) = \frac{\epsilon}{\Sigma}\frac{\ln T}{T} \tag{B4}$$

with logarithmic accuracy in T. If $T > \tau_*$, then the estimation for the first summand is less than (B4). The second summand on the right-hand side of (B3) is a viscous correction and it is parametrically small; see Eq. (B7). Thus, our consideration leads to the conclusion that the overall integral (25) is accumulated at times $\tau \sim 1$, that is, $t \sim 1/\Sigma$ for dimensional variables.

Next, let us evaluate the correction to the asymptotic value ϵ/Σ of the Reynolds stress. The deviation is determined by the integral in (26). One has $\sqrt{\lambda} \approx \tau\sin\theta|\cos\phi|$ at large times $\tau \gg 1$ and thus the first part of the integral is

$$\frac{5\gamma}{8\pi}\int_0^\pi \sin\theta\,d\theta\int_0^{2\pi}d\phi\int_0^{\tau_*}\frac{\sqrt{\lambda}\,d\tau}{(1+\gamma\Lambda)^{7/2}} \approx \frac{5\gamma}{8\pi}\int_0^\pi d\theta\int_0^{2\pi}d\phi\int_0^{\tau_*}d\tau\,\tau\sin^2\theta|\cos\phi| = \frac{5}{4}\gamma^{1/3}. \tag{B5}$$

If $\tau \gg \tau_*$, the denominator in (26) becomes large and it leads to domination of the domain with $|\cos\phi| \ll 1$. If $\tau \ll 1/\gamma$ and $|\cos\phi| \ll 1$, one has according to (B1) and (B3)

$$\frac{\sqrt{\lambda}\sin\theta\,d\phi}{(1+\gamma\Lambda)^{7/2}} \approx \frac{\cos^2\theta\sqrt{\zeta^2+1}\,d\zeta}{\tau(1+\mu^2)^{7/2}} \approx \frac{3}{\gamma\tau^2}\frac{|\mu|\,d\mu}{(1+\mu^2)^{7/2}}, \tag{B6}$$

where $\mu = \sqrt{\gamma\tau/3}\,|\cos\theta|\,(\zeta + \frac{1}{2}\tan\theta)$. Thus the next part of the integral is

$$\frac{5\gamma}{8\pi}\int_0^\pi \sin\theta\,d\theta\int_0^{2\pi}d\phi\int_{\tau_*}^{1/\gamma}\frac{\sqrt{\lambda}\,d\tau}{(1+\gamma\Lambda)^{7/2}} \approx \frac{3}{2}\int_{\tau_*}^{1/\gamma}\frac{d\tau}{\tau^2} = \frac{3}{2}\gamma^{1/3}, \tag{B7}$$

which coincides with (B5) by an order of magnitude. If follows from (B5) and (B7) that the integral in (26) is accumulated at times $\tau \sim \tau_*$. The physical time corresponding to τ_* is $t_* \sim (\Sigma^2\nu k_f^2)^{-1/3}$ and it can be found from the estimation $\nu\int_0^{t_*} dt\,\mathbf{k}'^2(t) \sim 1$.

Finally, let us evaluate the averaged kinetic energy $\langle \boldsymbol{u}^2\rangle$ per unit mass stored in the small-scale turbulent pulsations:

$$\langle \boldsymbol{u}^2\rangle = \sum_{s=\pm1}\int\frac{d^3k}{(2\pi)^3}|a_{\mathbf{k}s}|^2 = 2\epsilon\int\frac{d^3k}{(2\pi)^3}\int_{-\infty}^0 d\tau\,\chi(\mathbf{k}'(\tau))\frac{k'(\tau)}{k}\exp\left(-2\nu\int_\tau^0 dt'k'^2(t')\right). \tag{B8}$$

Analogously to (25), we get

$$\langle \boldsymbol{u}^2\rangle = \frac{2\epsilon}{\Sigma}\int\frac{d^3k}{(2\pi)^3}\chi(\mathbf{k})\int_0^\infty\frac{d\tau}{\sqrt{\lambda}}\exp(-\gamma k^2\Lambda). \tag{B9}$$

To make further estimations, we adopt the Gaussian isotropic form of the correlation function of the external force (3) and obtain

$$\langle \boldsymbol{u}^2 \rangle = \frac{\epsilon}{\Sigma} \int_0^{\pi} \frac{\sin\theta\, d\theta}{2\pi} \int_0^{2\pi} d\phi \int_0^{\infty} \frac{d\tau}{\sqrt{\lambda}(1+\gamma\Lambda)^{5/2}}. \tag{B10}$$

Now we divide the time integration interval $(0, \infty)$ into three intervals $(0, \tau_*)$, $(\tau_*, 1/\gamma)$, and $(1/\gamma, \infty)$. The integrals over the first and second intervals give the main contribution to (B10), and we arrive at the result

$$\langle \boldsymbol{u}^2 \rangle \approx \frac{\epsilon \ln^2 \gamma}{3\Sigma}. \tag{B11}$$

Note that the logarithmic dependence of (B11) on γ is determined by the viscous timescale $\tau \sim 1/\gamma$, that is, $t \sim 1/\nu k_f^2$ in terms of dimensional time. Note that the mean velocity squared (B11) is parametrically less than its value in the two-dimensional case, where $\langle \boldsymbol{u}^2 \rangle \sim \epsilon/\nu k_f^2$ and it is accumulated at the same timescale $t \sim 1/\nu k_f^2$ [6].

[1] Uriel Frisch, *Turbulence: The legacy of A.N. Kolmogorov* (Cambridge University Press, Cambridge, 1995).
[2] G. Boffetta and R. E. Ecke, Two-dimensional turbulence, Annu. Rev. Fluid Mech. **44**, 427 (2012).
[3] M. Chertkov, C. Connaughton, I. Kolokolov, and V. Lebedev, Dynamics of Energy Condensation in Two-Dimensional Turbulence, Phys. Rev. Lett. **99**, 084501 (2007).
[4] J. Laurie, G. Boffetta, G. Falkovich, I. Kolokolov, and V. Lebedev, Universal Profile of the Vortex Condensate in Two-Dimensional Turbulence, Phys. Rev. Lett. **113**, 254503 (2014).
[5] I. V. Kolokolov and V. V. Lebedev, Structure of coherent vortices generated by the inverse cascade of two-dimensional turbulence in a finite box, Phys. Rev. E **93**, 033104 (2016).
[6] I. V. Kolokolov and V. V. Lebedev, Velocity statistics inside coherent vortices generated by the inverse cascade of 2-d turbulence, J. Fluid Mech. **809**, R2 (2016).
[7] A. V. Orlov, M. Yu. Brazhnikov, and A. A. Levchenko, Large-scale coherent vortex formation in two-dimensional turbulence, JETP Lett. **107**, 157 (2018).
[8] A. Celani, S. Musacchio, and D. Vincenzi, Turbulence in More Than Two and Less Than Three Dimensions, Phys. Rev. Lett. **104**, 184506 (2010).
[9] S. Musacchio and G. Boffetta, Condensate in quasi-two-dimensional turbulence, Phys. Rev. Fluids **4**, 022602 (2019).
[10] A. van Kan and A. Alexakis, Condensates in thin-layer turbulence, J. Fluid Mech. **864**, 490 (2019).
[11] N. Francois, H. Xia, H. Punzmann, and M. Shats, Inverse Energy Cascade and Emergence of Large Coherent Vortices in Turbulence Driven by Faraday Waves, Phys. Rev. Lett. **110**, 194501 (2013).
[12] E. Deusebio, G. Boffetta, E. Lindborg, and S. Musacchio, Dimensional transition in rotating turbulence, Phys. Rev. E **90**, 023005 (2014).
[13] G. Schubert, *Treatise on Geophysics*, Vol. 8, Core Dynamics (Elsevier, Amsterdam, 2015).
[14] K. Seshasayanan and A. Alexakis, Condensates in rotating turbulent flows, J. Fluid Mech. **841**, 434 (2018).
[15] L. Biferale, F. Bonaccorso, I. M. Mazzitelli, M. A. T. van Hinsberg, A. S. Lanotte, S. Musacchio, P. Perlekar, and F. Toschi, Coherent Structures and Extreme Events in Rotating Multiphase Turbulent Flows, Phys. Rev. X **6**, 041036 (2016).
[16] A. Campagne, B. Gallet, F. Moisy, and P.-P. Cortet, Disentangling inertial waves from eddy turbulence in a forced rotating-turbulence experiment, Phys. Rev. E **91**, 043016 (2015).
[17] A. Campagne, B. Gallet, F. Moisy, and P.-P. Cortet, Direct and inverse energy cascades in a forced rotating turbulence experiment, Phys. Fluids **26**, 125112 (2014).
[18] B. Gallet, A. Campagne, P.-P. Cortet, and F. Moisy, Scale-dependent cyclone-anticyclone asymmetry in a forced rotating turbulence experiment, Phys. Fluids **26**, 035108 (2014).

[19] P. D. Mininni, A. Alexakis, and A. Pouquet, Scale interactions and scaling laws in rotating flows at moderate Rossby numbers and large Reynolds numbers, Phys. Fluids **21**, 015108 (2009).
[20] H. P. Greenspan, *The Theory of Rotating Fluids* (Cambridge University Press, Cambridge, 1968).
[21] A. Salhi and C. Cambon, An analysis of rotating shear flow using linear theory and DNS and LES results, J. Fluid Mech. **347**, 171 (1997).
[22] S. Galtier, Weak inertial-wave turbulence theory, Phys. Rev. E **68**, 015301(R) (2003).
[23] Y. Zhou, A phenomenological treatment of rotating turbulence, Phys. Fluids **7**, 2092 (1995).
[24] E. Yarom and E. Sharon, Experimental observation of steady inertial wave turbulence in deep rotating flows, Nat. Phys. **10**, 510 (2014).
[25] S. Nazarenko, N. K.-R. Kevlahan, and B. Dubrulle, Nonlinear RDT theory of near-wall turbulence, Physica D **139**, 158 (2000).
[26] T. Miyazaki and J. C. R. Hunt, Linear and nonlinear interactions between a columnar vortex and external turbulence, J. Fluid Mech. **402**, 349 (2000).